Experimental and Numerical Assessment of Board-level Temperature Cycling Performance for Eutectic and Pb-free windows-Chip-Scale-Package (wCSP)

Wei Sun, W. H. Zhu, F. X. Che, C. K. Wang, Anthony Y.S. Sun and H. B. Tan
United Test & Assembly Center Ltd (UTAC)
Packaging Analysis & Design Center
5 Serangoon North Ave 5, Singapore, 554916
Email: Sun_Wei@sg.utacgroup.com Tel: +65-65511345

Abstract

This paper examines the board-level solder joint reliability of UTAC's windows-Chip-Scale-Package (wCSP) under temperature cycling (TC) condition, both experimentally and numerically. Five legs of wCSP test vehicles were assembled with different solder ball sizes, mold compound materials and solder materials, i.e., eutectic Pb-Sn and Sn3Ag0.5Cu. Those assemblies were subject to TC condition using UTAC internal TC chamber and data collection system. TC condition was specified using the widely used industry standard, which is –40C~125C with 15mins ramp/dwell. For the numerical study, Darveaux's approach, which uses Anand visco-plasticity constitutive model plus fracture mechanics based fatigue model, was used for legs with eutectic 62Sn36Pb2Ag solders; while for Pb-free legs, various publicly available Pb-free constitutive and fatigue models were examined to see their prediction accuracy.

Introduction

Solder joint reliability under cyclic temperature changes has always been a concern due to the loading exerted by CTE (coefficient of thermal expansion) mismatch between package and PCB. With the increasing complexity of package structure and variety of material combination, such TC concern should be addressed as early as possible in the new package development process.

For the past several decades, eutectic Pb-Sn solder has been widely used. As long as the package is properly designed, satisfactory solder joint reliability can be achieved.

In the design stage, it is desirable to use simulation tool to predict the solder joint reliability not only in a qualitative way, but also in a quantitative way [1]. A lot of efforts have been put into this prediction model. Based on extensive characterization of solder materials, board-level TC experiments and the failure mechanisms observed, various prediction models using finite element simulation were proposed and verified by experiments. Among them, Darveaux's [2] visco-plasticity constitutive model plus his fracture mechanics based fatigue model is more popular than others due to its ease of implementation and is well known for its prediction accuracy.

However, the transition from Pb-based solder to Pb-free solders, driven by environmental concerns, makes it difficult to give an accurate prediction as in the age of eutectic Pb-Sn solder. This is because Pb-free solders have different mechanical characteristics. In order to establish an accurate prediction model for Pb-free solder, many researchers have conducted material characterization on various Pb-free solders (with different compositions) and proposed the corresponding fatigue models [3, 5-7]. Some of those Pb-free constitutive models and fatigue models are available in the public domain. This paper will use wCSP as the test vehicle to examine the various available Pb-free constitutive and fatigue models. For comparison purpose, eutectic legs were also included in the evaluation matrix and Darveaux's constitutive and fatigue models are used for prediction.

Test Vehicle Description

A schematic picture of UTAC single-die wCSP package is shown in Figure 1. The die is facing downwards and attached by die attach film to the substrate. The die used in actual application usually is a DRAM die, whose pads are located in the center of the die (in the case without redistribution layer). Wirebonding is done through the windows channel in the substrate to the bottom metal layer. This design allows maximum electrical performance due to its minimum path length from die to solder joints.

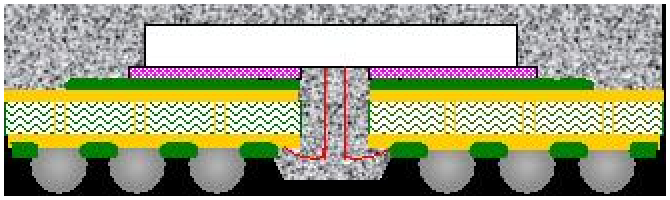

Figure 1: Schematic picture of single-die wCSP

As for the test vehicle used in the experiments, mechanical die is used with daisy-chained substrate to form the complete circuit with Cu traces on the test board for continuous failure monitoring. The die size used is of typical size as a normal DRAM die. A typical test board assembly is shown below.

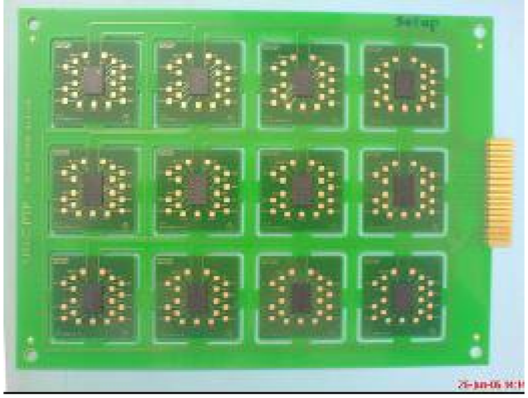

Figure 2: Test board with wCSP packages

The assembled PCB assemblies were slotted into UTAC internal TC chamber for in-situ monitoring. Once there is failure based on the failure criterion (300 ohms) pre-defined, the data collection computer can automatically log it down.

The TC profile is optimized before conducting the experiments so that the temperature profile meets the requirement for 15mins ramp/dwell.

Figure 3: UTAC in-house TC chamber with in-situ monitoring system

Experiment Matrix

Totally 5 different legs were tested. Of them two solder ball sizes, 0.4mm and 0.45mm in diameter, and two mold compounds, A and B, were included to study the effect of mold compound material, solder ball materials and size on solder joint TC fatigue performance. Compared with mold compound B, A has lower modulus and slightly higher CTE. The evaluation matrix is shown in Table 1.

Table 1: Experiment matrix for wCSP board-level TC test

Leg No	Package type	Solder type /size (mm)	EMC
5	wCSP-1die	62Sn36Pb2Ag/0.40	A
6	wCSP-1die	Sn3Ag0.5Cu/0.40	A
9	wCSP-1die	62Sn36Pb2Ag/0.45	A
10	wCSP-1die	Sn3Ag0.5Cu/0.45	A
11	wCSP-1die	Sn3Ag0.5Cu/0.45	B

Experimental Results and Discussion

Up to 3000X, all the 5 test legs reached full failure. The failure data was collected and analyzed. The characteristic lives for all the five legs were calculated and shown in Table 2. A more clear comparison of characteristic lives among the 5 legs is shown in Figure 4.

The failure data was analyzed to find out which location see most frequent failures. Since failure isolation was only done after completion of experiments, so the most frequent failure site should also be the most critical/vulnerable site. Analysis shows that the critical location is at the package corner, circled by pink color, as shown in Figure 5.

Table 2: TC results for all the 5 legs

Leg	First Failure	Last Failure	63.2% life
5	1696	2193	1994
6	1353	2586	2288
9	1198	2341	1974
10	519	2986	2313
11	1198	2785	2292

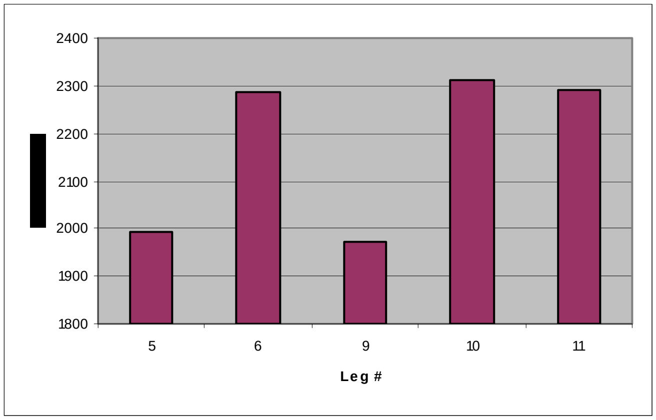

Figure 4: Characteristic lives for all the five legs

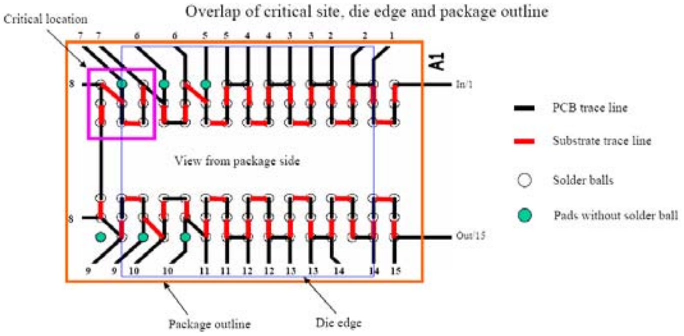

Figure 5: Critical solder joint locations for wCSP 84B test vehicle

From the results shown in above Tables and Figures, it is observed that:

1. Almost all the units across the 5 legs passed 1000X except that two units in leg 10 failed early before 1000X, at 519X and 963X, respectively. Early failure could be due to SMT assembly defect and may not be representative of the actual application where end user will optimize the SMT assembly process.
2. Eutectic Pb-Sn legs, leg 5 and leg 9, have a characteristic fatigue life of a little bit below 2000X; while Pb-free legs, namely leg 6, leg 10 and leg 11, have a characteristic fatigue life which is around 2300X. This shows that Pb-free solder Sn3Ag0.5Cu apparently outperforms eutectic Pb-Sn in terms of TC fatigue durability.
3. Leg 10 with Pb-free solder and mold compound A yields the best solder joint reliability among all the legs. Talking about the impact of molding compound on solder joint reliability, A and B has comparable solder joint characteristic fatigue lives, with A yielding slightly better result.

4. Theoretically, legs with larger solder ball size should have better solder joint reliability than their counterparts with smaller solder balls. Since solder joint fatigue failure is well known to be mainly due to shearing, simply assume that the shear strain follows:

$$\gamma = \frac{\Delta CTE \times L \times \Delta T}{H} \tag{1}$$

Where H is the solder joint height. The larger the solder ball size, the higher the solder joint after reflow. Under the same TC condition, a larger solder ball size will result in lower shear strain, thus yielding better TC performance. While the results comparison between leg 6 and leg 11 does conform to above theory, the conflict between the results from leg 5 and leg 9 and the above theory will be explained in detail later in the next section.

Failure Analysis

One failed unit was cross-sectioned to see the failure mode. As shown in Figure 6, the failure is solder joint crack at the component side. This finding is consistent with the literature [3] and confirms that the solder joint/component side interface is more prone to failure than the PCB side under board-level TC.

Two units, one from leg 5 and one from leg 9, were cross-sectioned to investigate the cause for the observation that leg 5 (solder ball size 0.4mm) has a better TC reliability than leg 9 (solder ball size 0.45mm). As mentioned earlier, larger solder ball size is expected to have a better TC performance than small ball size.

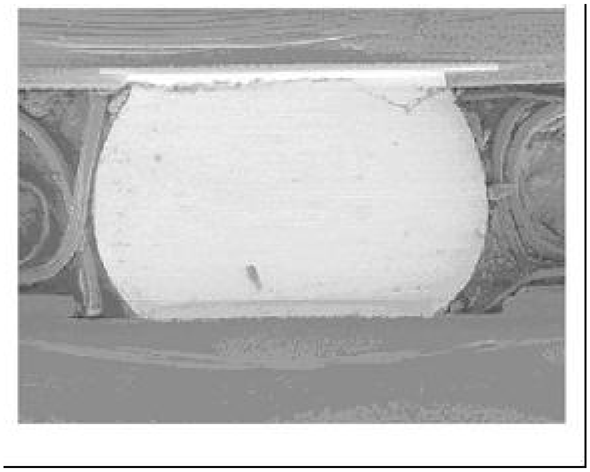

Figure 6: Solder joint crack at the component side

The cross-section direction and cross-sectioned solder joints are shown in Figure 7. Totally 12 solder joints were cross-sectioned for each of the two units. It was found that 9 out of 12 solder joints of the unit from leg 5 have large void inside the solder joints; while for the unit of leg 9, only 1 out of 12 joints was found to have void. A typical void in solder joint is shown in Figure 8.

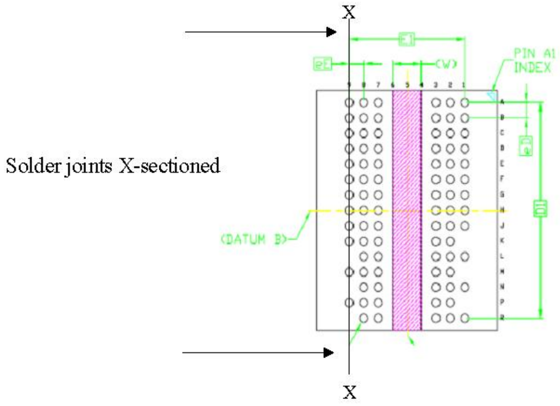

Figure 7: Cross-section direction and solder joints

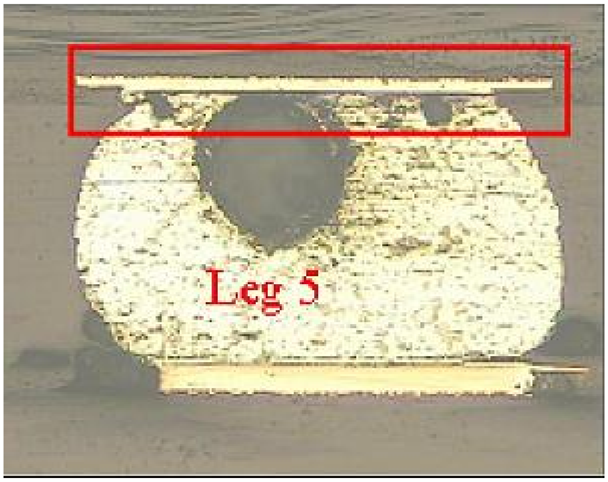

Figure 8: Void in solder joint

As many more voids are found on the solder joints of leg 5 than leg 9, with the presence of void, the solder joint size of leg 5 can be identical with that of leg 9. Moreover, the voids mainly lie on the crack propagation path, thus helping to reduce the fatigue crack growth (because stress intensity factor for sharp crack is infinity while the stress intensity factor for void (if taken as circular shape) is around 2, so with the presence of void, it may reduce the speed of crack propagation)

Simulation-Objective and Matrix

The objective of current simulation is to 1) investigate the correlations between simulation results and experimental results; 2) perform a study of lead-free solder joint modeling using various constitutive models and fatigue correlations available in the public domain and select the best combination for future lead-free solder modeling; 3) explore the feasibility of quarter model (wCSP under current study exhibits a non-symmetric array of solder balls as shown in Figure 7)

The simulation matrix based on above objectives is shown in Table 3.

Table 3: Matrix for the simulation study

Eva1 #	Solder	EMC	Model
#1	Pb-free/0.40	A	Full Model
#2	Pb-free/0.45	A	Full Model
#3	Pb-free/0.45	A	Quarter Model
#4	Pb-free/0.45	B	Full Model
#5	Eutectic/0.40	A	Full Model
#6	Eutectic/0.45	A	Full Model

Simulation- Constitutive and Fatigue Models

For eutectic Pb-Sn solder joint modeling, Darveaux [2] modified Anand visco-plastic constitutive model and his fracture mechanics based fatigue life correlation model is used. Anand's model can be directly implemented in ANSYS software and its nine constants, from C1 to C9, are shown in Table 4 [2].

Table 4: Anand's constants for eutectic solder [2]

C1	So	12.41	Initial value of deformation resistance
C2	Q/k	9400	Activation energy
C3	A	4e06	Pre-exponential factor
C4	ξ	1.5	Multiplier stress
C5	m	0.303	Strain rate sensitivity of stress
C6	ho	1379	Hardening constant
C7	s^	13.79	Coefficient for deformation resistance saturation value
C8	n	0.07	Strain rate sensitivity of saturation (deformation resistance) value
C9	a	1.3	Strain rate sensitivity of hardening

Other material properties of the eutectic Pb-Sn solder are listed in Table 5.

Table 5: Other material properties for eutectic older [4]

E (MPa)	75790-152T (degree K)
ν	0.35
CTE (ppm/K)	24.5

For Pb-free solder joint, currently in the public domain there is no such a constitutive model and fatigue life correlation model that can predict the solder joint fatigue behavior as accurate as Darveaux model. So current simulation study will explore the Pb-free solder constitutive models and fatigue correlation models available in the public domain. Schubert et al. [5] proposed the use of hyperbolic sine function to describe the creep behavior of Pb-free solder Sn4Ag0.5Cu while Wiese et al. [6] described the steady-state creep behavior of Sn3.8Ag0.7Cu, Sn3.5Ag0.75Cu and Sn3.5Ag0.5Cu using a double power law constitutive equation. Table 5 shows the constitutive equations by Schubert et al. and Wiese et al.

Table 6: Constitutive equations for Pb-free solders

Solder composition	Constitutive equation
Sn4Ag0.5Cu (Wiese et al. [6])	$\dot{\varepsilon} = 4\times10^{-7}\exp\left(\frac{-3223}{T\left(^{o}K\right)}\right)\left(\frac{\sigma}{1MPa}\right)^{3} + 1\times10^{-12}\exp\left(\frac{-7348}{T\left(^{o}K\right)}\right)\left(\frac{\sigma}{1MPa}\right)^{12}$
Sn3.8Ag0.7Cu Sn3.5Ag0.75Cu Sn3.5Ag0.5Cu (Schubert et al. [5])	$\dot{\varepsilon} = 277984\left[\sinh(0.02447\sigma)\right]^{6.41}\times \exp\left(\frac{-6500}{T\left(^{o}K\right)}\right)$

Other material properties of the Pb-free solders are listed in Table 7 [5,6].

E (MPa)	59533-66.667T (degree K) (Wiese et al.) 61251-58.5T (degree K) (Schubert et al.)
ν	0.36
CTE (ppm/K)	20.0

For the fatigue life prediction models, Darveaux's fracture mechanics based model shown below is used for eutectic Pb-Sn solder.

$$\text{Crack Initiation: } N_o = K_1 \Delta W_{ave}^{K2} \qquad (2)$$

$$\text{Crack Growth: } \frac{da}{dN} = K_3 \Delta W_{ave}^{K4} \qquad (3)$$

Where K_1 to K_4 are the constants for above model and can be found in [2].

For Pb-free solders, Syed proposed both accumulated creep strain based and creep energy density based fatigue prediction models in his work [7].

Table 8: Syed's fatigue correlation model for Schubert's hyperbolic sine constitutive equation [7]

Acc. Creep Strain	$N_{mean} = \left(0.0513\varepsilon_{acc}\right)^{-1}$
Creep Energy Density	$N_{mean} = \left(0.0019w_{acc}\right)^{-1}$

Table 9: Syed's fatigue correlation model for Wiese's double power constitutive equation [7]

Acc. Creep Strain	$N_{mean} = \left(0.0468\varepsilon_{acc}\right)^{-1}$
Creep Energy Density	$N_{mean} = \left(0.0015w_{acc}\right)^{-1}$

It should be noted that in Table 8 and 9, N_f is the mean life. According to Syed, characteristic life can be approximated based on below equation when β in the two-parameter Weibull plot is equal to 10.

$$N_{cha} = 1.05\times N_{mean} \qquad (4)$$

Schubert [5] also proposed his energy and strain based fatigue models in his work. His models are shown in Table 10.

Table 10: Schubert's fatigue correlation model for his hyperbolic sine constitutive equation

Acc. Creep Strain	$N_{cha} = 4.5\varepsilon_{acc}^{(-1.295)}$
Creep Energy Density	$N_{cha} = 345w_{acc}^{(-1.02)}$

For Pb-free solders both researchers' energy and strain based fatigue models will be investigated. This is mainly to see which constitutive model plus fatigue correlation model can lead to best prediction accuracy.

Simulation-FE Mesh and Boundary Conditions

FE models were set-up based on the simulation matrix in Table 3. Figure 9 shows a typical mesh for full model.

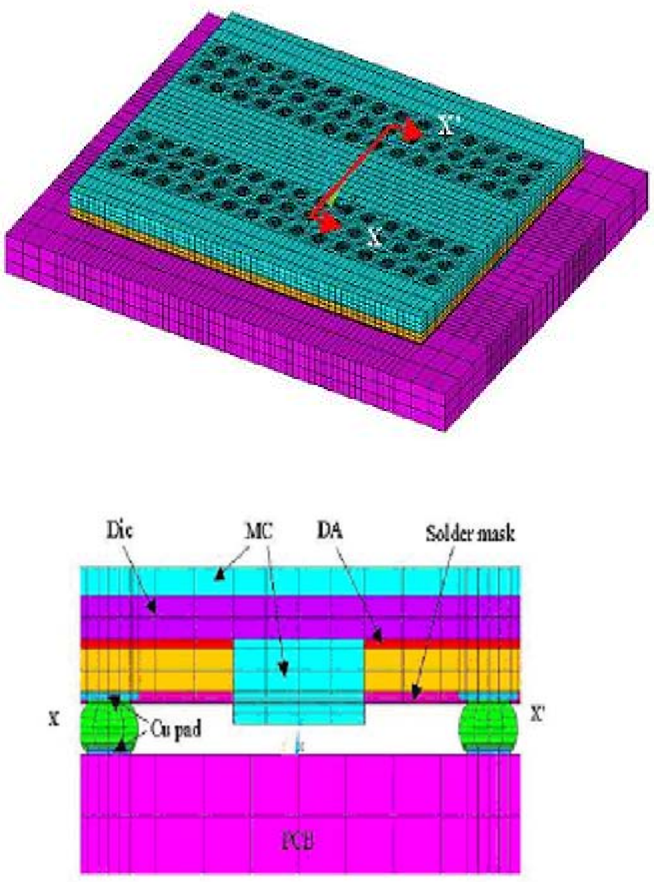

Figure 9: Typical FE mesh for the TC simulation

Note that for the fully model, there is some difficulty in applying the boundary conditions. In light of this, minimum boundary conditions should be applied onto the model. Therefore, 5 nodes in the center of the PCB bottom surface are fixed to prevent rigid body motion.

Simulation-Results and Discussion for Eutectic Pb-Sn Legs

The comparison between simulation prediction and experimental results is shown in Figure 10. It is seen that simulated characteristic life for leg 5 is 2100X. Compared to actual test result, which is 1994X, simulation over predicts the fatigue life by 5.32%. Simulated characteristic life for leg 9 is 2921X. Compared to actual test result, which is 1974X, simulation over predicts the fatigue life by 47.9%.

As mentioned earlier in the experiment results and failure analysis sections, leg 9 by right should have a better TC performance than leg 5. However, due to the excessive existence of voids in leg 5, the difference in TC performance between leg 5 and 9 is blurred. In light of the less voids in leg 9, leg 9 should be more representative of the case where SMT assembly has been properly conducted and solder joint formation is good. Thus the simulation prediction accuracy should be judged by comparing the simulation and experimental results of leg 9.

It is also observed from simulation that when the solder ball size is larger, the TC life is also longer.

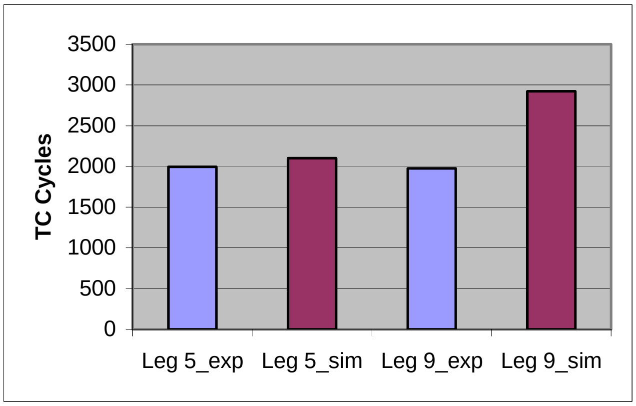

Figure 10: Results comparison between simulation and experiments

Simulation-Results and Discussion for Pb-free Legs

Table 11 shows the prediction accuracy for all the 3 Pb-free legs. The accuracy in current context is defined in Equation (5). Apparently Schubert's hyperbolic sine constitutive equation plus his energy based fatigue prediction model gives the best prediction accuracy. It is also seen that mostly simulations tend to over predict solder joint fatigue life with just one exceptional case where solder joint fatigue life is under predicted. It should be noted that although current study shows that Schubert's hyperbolic sine equation and his energy approach yields the best prediction accuracy for Pb-free solder joints, this does not mean that this combination will definitely give similar accuracy for all kinds of packages. Additional TC tests using different package size, die size, package type, etc are needed in the future to find out or curve fit the best fatigue correlation model.

$$Accuracy = \frac{Cycle\_prediction - Cycle\_actual}{Cycle\_actual} \times 100\% \quad (5)$$

Table 11: Prediction accuracy for Pb-free legs

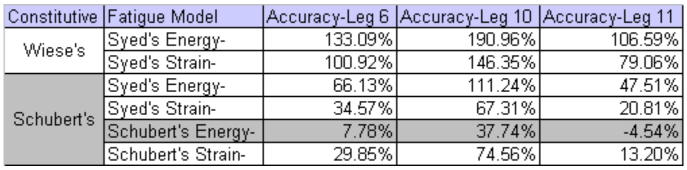

Constitutive	Fatigue Model	Accuracy-Leg 6	Accuracy-Leg 10	Accuracy-Leg 11
Wiese's	Syed's Energy-	133.09%	190.96%	106.59%
	Syed's Strain-	100.92%	146.35%	79.06%
Schubert's	Syed's Energy-	66.13%	111.24%	47.51%
	Syed's Strain-	34.57%	67.31%	20.81%
	Schubert's Energy-	7.78%	37.74%	-4.54%
	Schubert's Strain-	29.85%	74.56%	13.20%

Simulation-Feasibility of Quarter Model for Prediction

It is noted that for the wCSP package under investigation, the solder joints do not exhibit a full array. As shown in Figure 7, six of ninety solder joints were depopulated. Such solder joint depopulation makes it doubtable to use quarter symmetric FE model to do the prediction. Therefore, the feasibility of using quarter FE model despite its non-quarter-symmetry nature is investigated. Simulation assumption is that the package is fully populated with solder balls, e.g. 90 balls. The results of this study can also show whether the missing balls have a significant effect on the overall solder joint reliability. For the comparison, leg 5 is simulated. Results from quarter model and full model are to be compared.

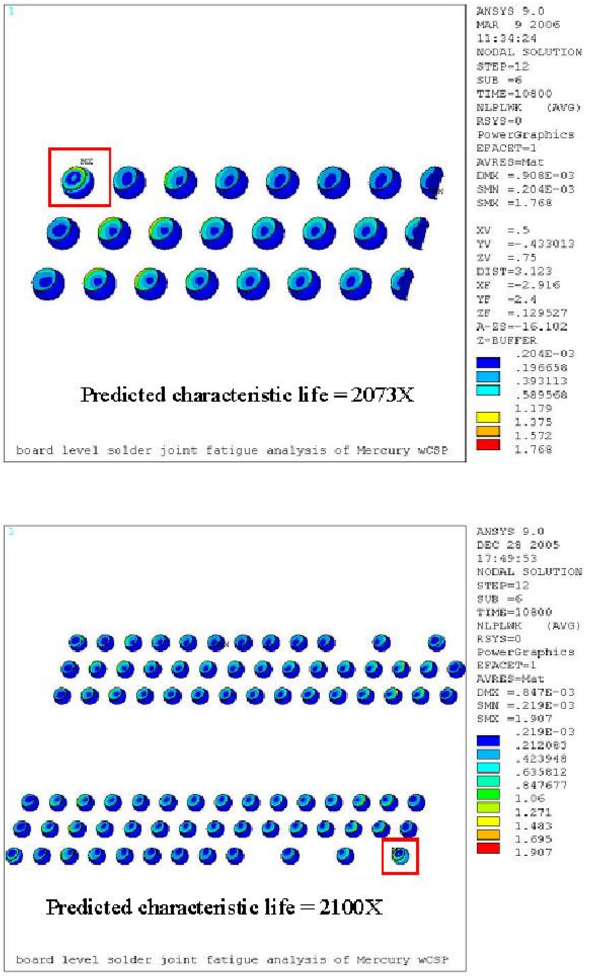

Figure 11: Results comparison between quarter and full models

From Figure 11, we can see that despite ignoring the missing balls, quarter model predicts the same critical location as the full model. It is also interesting to see that the quarter model, which assumes more solder joints, predicts a little bit less TC cycles than the full model. An explanation is that the missing balls in full model make the loading from CTE mismatch more evenly distributed among critical and other balls so that the most critical solder ball can experience a less severe loading than that in quarter model.

Conclusions

Board-level TC experiments were done for UTAC single-die wCSP packages. Experimental results showed that Pb-free Sn3Ag0.5Cu solder apparently outperforms its eutectic Pb-Sn counterpart. Both eutectic and Pb-free wCSP legs perform far beyond the industry's TC expectation, which is 1000X under –40C~125C with 15mins ramp/dwell. It is found that larger solder ball size and low modulus mold compound tend to give better TC performance.

Numerical simulation results showed that Darveaux's approach over predicts the TC performance for eutectic Pb-Sn wCSP by about 48%. For Pb-free legs, it is found that Schubert's hyperbolic sine constitutive model plus his creep strain energy based fatigue correlation model can give the best prediction accuracy. However, more experiments are needed in the future to further test whether this combination still can give best prediction accuracy for other packages. Simulation also shows that despite the non-quarter-symmetry nature of 84 ball wCSP, using quarter model for modeling still give very similar result as full model, which means quarter model can be used for future modeling efforts to save model setup and computational time.

Acknowledgments

The authors would like to thank their former colleague, Mr Lim Beng Kuan, for conducting the experiments. Thanks should also be given to UTAC R&D management for their support.

References

1. T. Y. Tee, H. S. Ng and Z. W. Zhong, "Design for Package and Board Level Reliability with CAE", *Inivted Paper, SEMICON Advanced Packaging Technology Symposium, Singapore, 2003*, pp. 59-67
2. R. Darveaux, "Effect of Simulation Methodology on Solder Joint Crack Growth Correlation", *Proceedings of ECTC2000*, pp.1048-1058
3. Q. Zhang et al., "Systematic Study on Thermo-Mechanical Durability of Pb-free Assemblies: Experiments and FE Analysis", *Journal of Electronic Packaging, December 2005, Vol. 127*, pp.415-429
4. Bret A Zahn, "Finite Element Based Solder Joint Fatigue Life Predictions for a Same Die Size-Stacked-Chip Scale-Ball Grid Array Package", *SEMICON West 2002*, pp.274-284
5. A. Schubert et al., "Fatigue Life Models for SnAgCu and SnPb Solder Joints Evaluated by Experiments and Simulation", *Proceedings of ECTC2003*, pp.603-610

6. S. Wiese and E. Meusel, “Characterization of Lead-Free Solders in Flip Chip Joints”, *Journal of Electronic Packaging, December 2003, Vol. 125*, pp.531-538
7. Ahmer Syed, “Accumulated Creep Strain and Energy Density Based Thermal Fatigue Life Prediction Models for SnAgCu Solder Joints”, *Proceedings of ECTC2004*, pp.737-746